JOURNAL OF APPLIED POLYMER SCIENCE VOL. 18, PP. 2997–3018 (1974)

Rheological Phenomena in Polymerization Reactors: Rheological Properties and Flow Patterns Around Agitators in Polystyrene–Styrene Solutions

YOSHIAKI IDE and JAMES L. WHITE, *Department of Chemical and Metallurgical Engineering, The University of Tennessee, Knoxville, Tennessee 37916*

Synopsis

The rheological properties (viscosity and principal normal stress difference) of polystyrene–styrene solutions at concentrations of 15, 20, 30, 35, 43, 50 and 57 wt-% have been measured at 60°C. The flow patterns around a sphere, disc, turbine, and screw propellers in such solutions have also been determined. The second-order fluid theory of viscoelastic fluids containing parameters determined from our rheological measurements has been used to predict the flow patterns about the sphere. The observed flow patterns are in good agreement with the theoretical predictions based upon externally measured rheological properties. The implications of this study to the behavior of batch and CSTR polymerization reactors are discussed.

INTRODUCTION

Industrial continuous-addition polymerization processes are frequently carried out in solution or bulk. Such processes generally involve the flow of concentrated polymer solutions through complex geometries and around agitators. As these polymer solutions are viscoelastic fluids, one must expect that polymerizing systems will exhibit the rather complicated flow behavior typical of these systems. Polymer solutions exhibit non-Newtonian viscosity, normal stresses, elastic recoil, and stress overshoot in the relatively simple shearing motions exhibited in viscometers. It would be expected that homogeneous polymerizing mixtures flowing through industrial reactors would exhibit flow patterns similar to those derived from the theory of nonlinear viscoelastic fluids for such geometries and that these will influence reactor performance. The qualitatively different flow patterns which must be exhibited by viscoelastic polymerizing systems as opposed to Newtonian low molecular weight reacting fluids have generally been ignored.

The stirred tank reactor is a reactor type of major importance in polymerization processes. This makes the character of flow patterns around agitators in such tanks of considerable importance. There is an extensive literature on the subject for Newtonian fluids.[1–8] While there have been several experimental studies of rotating spheres, discs, and agitators in polymer solutions,[9–19] they have been limited to the polyacrylamide–water–

glycerol and aqueous carboxymethyl cellulose systems. None has considered solutions of a polymer dissolved in its monomer, nor has the influence of polymer concentration been investigated for any polymer–solvent system.

It is the purpose of this paper to experimentally investigate the rheological properties and flow patterns around agitators in an important bulk polymerizing system, polystyrene–styrene. This is an important system to study because of the great importance of polystyrene as an engineering plastic.[20] The dependence of both rheological properties and flow patterns about various agitators upon concentration will be determined. We will contrast the observed flow patterns with a fluid mechanical theory containing experimentally determined rheological coefficients. Similar behavior would be expected in bulk polymerizing systems. This paper is part of two research programs: (i) to experimentally observe and theoretically analyze flow patterns during polymer processing operations[21,22] and (ii) to study polymerization reactor behavior.[23]

BACKGROUND

Theory of Viscoelastic Fluids

Our basic approach will be to consider the rheological properties of the polymer solution to be representable by the smooth, long duration flow asymptote of nonlinear viscoelastic fluid theory.[24–30] This may be expressed as follows:

$$\mathbf{\sigma} = -p\mathbf{I} + \sum \mathbf{M}_n \tag{1}$$

where

$$\mathbf{M}_1 = \omega_1\mathbf{B}_1 \tag{2a}$$

$$\mathbf{M}_2 = \omega_2\mathbf{B}_1^2 + \omega_3\mathbf{B}_2 \tag{2b}$$

$$\mathbf{M}_3 = \omega_4[tr\mathbf{B}_1^2]\mathbf{B}_1 + \omega_5(\mathbf{B}_1\mathbf{B}_2 + \mathbf{B}_2\mathbf{B}_1) + \omega_6\mathbf{B}_3 \tag{2c}$$

etc., where the ω_j are constant coefficients and the $\mathbf{B}_n$ are acceleration tensors defined by

$$\mathbf{B}_1' = (\nabla\mathbf{v}) + (\nabla\mathbf{v})^T \tag{3a}$$

$$\mathbf{B}_{n+1} = \frac{D}{Dt}\cdot\mathbf{B}_n - \nabla\mathbf{v}\cdot\mathbf{B}_n - \mathbf{B}_n\cdot\nabla\mathbf{v}. \tag{3b}$$

The term $\mathbf{M}_1$ is essentially the Newtonian fluid as developed by Stokes.[31,32] The sum of $\mathbf{M}_1$ and $\mathbf{M}_2$ is the second-order fluid.[25–27]

The coefficients ω_1, ω_3, and ω_6 are related to the relaxation modulus of linear viscoelasticity through the relations[26,27]

$$\omega_1 = \int_0^\infty G(s)ds \tag{4a}$$

$$\omega_3 = -\int_0^\infty sG(s)ds \tag{4b}$$

$$\omega_6 = \frac{1}{2}\int_0^\infty s^2G(s)ds. \tag{4c}$$

If one defines a characteristic relaxation time λ as the ratio of the first to the zeroth moment of $G(s)$, it follows that

$$\lambda = -\frac{\omega_3}{\omega_1}. \tag{5a}$$

The steady-state shear compliance J_e is given by

$$J_e = -\frac{\omega_3}{{\omega_1}^2}. \tag{5b}$$

The coefficients ω_1, ω_2, and ω_3 may be determined from low shear viscosity and normal stress measurements. Specifically,

$$\omega_1 = \eta = \lim_{\Gamma \to 0} \mu \tag{6a}$$

$$\omega_2 = \lim_{\Gamma \to 0} (N_2/\Gamma^2) \tag{6b}$$

$$\omega_3 = \lim_{\Gamma \to 0} [(-1)N_1/2\Gamma^2] \tag{6c}$$

where μ is the non-Newtonian shear viscosity, Γ is the shear rate, and N_1 and N_2 are the principal and second normal stress differences, respectively.

Rheological Properties of Polystyrene–Styrene Solutions

There have been numerous studies of the rheological properties of polystyrene solutions in various solvents.[33–41] However, few studies involving solutions in styrene[36,38] have been reported, and these involve viscosity measurements only. No data on viscoelastic properties of polystyrene–styrene solutions seem to exist.

Survey of Studies of Flow About Rotating Bodies

There is a long history of studies of flows around rotating objects in Newtonian fluids dating to Newton and Stokes. We restrict ourselves here to laminar flow which is nost important for high-viscosity systems. Jeffery[42] has shown from the Navier-Stokes equations that only in the case of a rotating infinite cylinder are the streamlines circles having their centers on the axis and their planes perpendicular to the axis. Circular streamlines also possible for more general types of agitators if centrifugal forces and inertia are neglected. The velocity field around a rotating cylinder was first derived by Stokes[31] who also determined the creeping flow velocity field about a rotating sphere in an infinite bath.[31] Jeffery[43] has studied creeping flow around a sphere nonconcentrically placed in a spherical container, while Brenner and Sonshine[44] have analyzed creeping flow around a rotating sphere in a cylindrical container. Jeffery[43] has determined the slow flow velocity field in the neighborhood of rotating oblate and prolate spheroids and a disc.

As first recognized by Stokes,[31] centrifugal forces interact with the velocity field in the case of a sphere and cause fluid to be drawn in at the poles and expelled at the equator. Stokes remarked: "In fact it is easy to see that from the excess of centrifugal forces in the neighborhood of the equator

of the revolving sphere the particles in that part will recede from the sphere, and approach it again in the neighborhood of the poles, and this circulating motion will be combined with a motion about the axis."[31]

The detailed character of these secondary flows were first computed by Bickley[45] in 1938 using a perturbation procedure. Similar secondary flows near a rotating infinite disc were found by Von Karman[46,47] with an exact solution of the Navier-Stokes equations and by Waters and King[48] for spheroids and a finite disc by applying Bickley's technique to Jeffery's solution.

There have also been attempts, albeit not as rigorous, by DeSouza and Pike,[8] among others, to model flow around a turbine in a finite tank. These solutions again show the dominant centrifugal fan effect. Experimental studies[1,2,4,7,8] at least qualitatively bear out all of these flow patterns. It must, of course, be realized that all rotating agitators do not give rise to radially outward flows, the most notable exception being the screw propeller[1,2,49] where the rotation drives fluid away axially.

Flow patterns around rotating agitators in viscoelastic fluids were first analyzed by Giesekus,[10,11] Thomas and Walters,[50] and Langlois[51] about a decade ago using Bickley's perturbation method. However, none of these authors cites Bickley, and it seems more likely that their approach was instead influenced by Green and Rivlin's study[52] (see also Langlois and Rivlin[53]) of the impossibility of rectilinear flow and the development of vortices in certain non-Newtonian fluids in an elliptical pipe.

Normal stresses like centrifugal forces are incompatible with laminar shearing flow around a sphere but tend, rather than expel the fluid radially outward at the equator, to draw the fluid in and induce effects of the type first described by Weissenberg.[54] Thus, depending upon the relative level of normal stresses and centrifugal forces, one may have secondary flows with opposite directions. This is brought out in the work of Giesekus and Thomas and Walters who also find that when the viscoelastic normal stress forces balance out the centrifugal forces, the secondary flow pattern breaks down into two distinct regions with the region closest to the sphere consisting of segregated vortices.

These flow patterns have been observed by Giesekus[10,11] and Walters and Savins.[12] These authors and Walters and Waters[12] and Ulbrecht and his co-workers[19] have described the possible application of torque and flow pattern measurements on a rotating sphere in an infinite bath to obtain viscoelastic properties of polymer solutions, and some measurements have been made. Palekar[55] has perturbated around Brenner and Sonshine's solution[44] for creeping flow about a rotating sphere in a cylinder and computed the secondary flows due to normal stresses (but not centrifugal forces). Walters et al.[12,56] have studied the influence of a spherical container on combined normal stress and centrifugal force induced flow patterns. The flow patterns induced in a viscoelastic fluid near an infinite rotating disc have been analyzed by Griffiths, Jones, and Walters,[14] and the finite disc problem has been worked out numerically by these authors and by Waters and King[48] using a perturbation procedure. The distinctive flow patterns near a disc

(which are similar to those around a sphere) have been observed by the former authors. Theoretical and experimental studies of flow patterns in related geometries such as cone-plate combinations,[10,11,57] combined cone-plate-hemispheres,[15] and a disc-in-cylinder[58,59] have been reported.

In addition to the flows discussed in the above paragraphs, secondary flows are observed in polymer fluids in various other geometries which may be used in polymerization reactors, especially flow near contractions[21,60–63] and conduits with noncircular cross sections.[11]

THEORY OF FLOW ABOUT ROTATING SPHERE

To determine flow patterns around the sphere in an infinite bath (Fig. 1), we will apply a perturbation procedure in a manner similar to that used by Bickley, Giesekus, Thomas and Walters, and Langlois as cited earlier. There are differences in our detailed formulation, though the results are equivalent. Equation (1) is substituted into Cauchy's low of motion:

$$\rho\left[\frac{\partial \mathbf{v}}{\partial t} + (\mathbf{v}\cdot\nabla\mathbf{v})\right] = \nabla\cdot\mathbf{\sigma} + \rho\mathbf{f}. \tag{7}$$

We proceed by expressing the velocity and pressure fields as a perturbation about the state of rest:

$$\begin{aligned} \mathbf{v} &= \epsilon\mathbf{v}^{(1)} + \epsilon^2\mathbf{v}^{(2)} + \epsilon^3\mathbf{v}^{(3)} + \dots \\ p &= \epsilon p^{(1)} + \epsilon^2 p^{(2)} + \epsilon^3 p^{(3)} + \dots \end{aligned} \tag{8}$$

If we equate terms of equal order in ϵ, we obtain (after neglecting transient and body force terms)

$$0 = \nabla p^{(1)} + \omega_1\nabla^2\mathbf{v}^{(1)} \tag{9a}$$

$$\rho(\mathbf{v}^{(1)}\cdot\nabla\mathbf{v}^{(1)}) - \omega_2\nabla\cdot B_1{}^{(1)2} - \omega_3\nabla\cdot B_2{}^{(1)} = -\nabla p^{(2)} + \omega_1\nabla^2\mathbf{v}^{(2)}. \tag{9b}$$

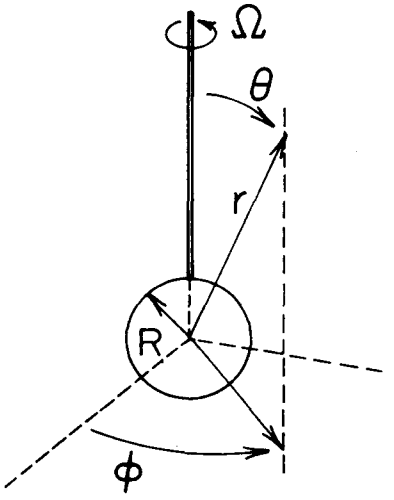

Fig. 1. Rotating sphere in an infinite bath.

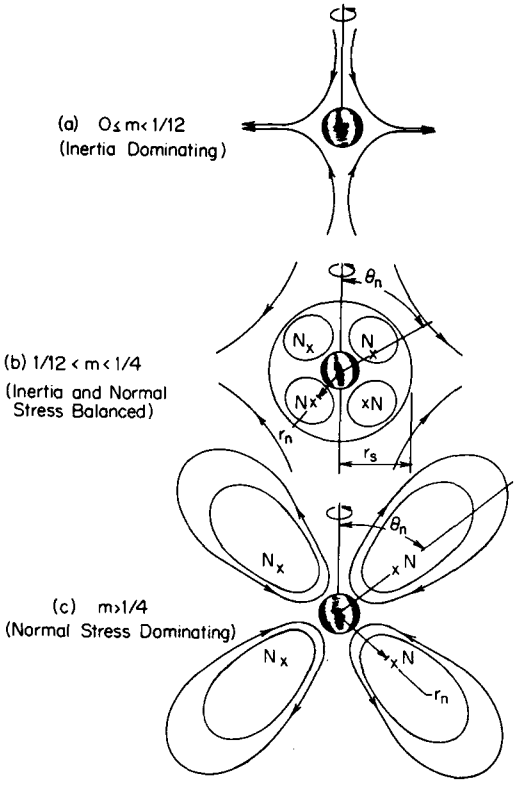

Fig. 2. The secondary flow patterns around a sphere for (a) low levels of viscoelasticity ($0 \leq m < {}^1/_{12}$), (b) intermediate (${}^1/_{12} < m < {}^1/_4$), and (c) high levels of viscoelasticity ($m > {}^1/_4$).

Equation (9a) is simply the creeping flow Navier-Stokes equation. For a sphere rotating about its axis in an infinite bath, the solution neglecting the effect of the axial rod which stations the rotor is (due originally to Stokes[32])

$$\mathbf{v}^{(1)} = R\Omega \sin\theta \left(\frac{R}{r}\right)^2 \mathbf{e}_\phi + 0\mathbf{e}_\theta + 0\mathbf{e}_r \tag{10}$$

where Ω is the angular velocity of the sphere, R is its radius, r is the distance from the center of the sphere to the particle of fluid in question, and θ is the angle measured from the polar of the sphere. The perturbed flow contains θ and r as well as a ϕ component. These components may be determined from eq. (9b) by eliminating $p^{(2)}$ from the θ and r components of the equations of motion and introducing the stream function $\psi^{(2)}$ defined by

$$v_r^{(2)} = -\frac{1}{r^2 \sin\theta}\frac{\partial\psi^{(2)}}{\partial\theta}; \quad v_\theta^{(2)} = +\frac{1}{r\sin\theta}\frac{\partial\psi^{(2)}}{\partial r}. \tag{11}$$

This leads to a nonhomogeneous biharmonic equation of form

$$\omega_1 E^4 \psi^{(2)} = \omega_1 \left(\frac{\partial^2}{\partial r^2} + \frac{1}{r^2} \frac{\partial^2}{\partial \theta^2} - \frac{\cot \theta}{r^2} \frac{\partial}{\partial \theta} \right)^2 \psi^{(2)}$$

$$= \left\{ 6\rho\Omega^2 R \left(\frac{R}{r} \right)^5 + \frac{144\, \omega_3 \Omega^2}{R} \left(1 - \frac{\omega_2}{\omega_3} \right) \left(\frac{R}{r} \right)^7 \right\} \sin^2\theta \cos\theta \quad (12)$$

which has the following solution (in dimensionless form):

$$\psi^{(2)*} = \frac{\psi^{(2)}}{R^3\Omega} = \frac{N_{\mathrm{Re}}[r^* - 1]^2}{8r^{*3}} [(1 - 4m)r^* - 8m] \sin^2\theta \cos\theta \quad (13)$$

where

$$N_{\mathrm{Re}} = \frac{R^2\Omega\rho}{\omega_1} \qquad m = \frac{N_{\mathrm{We}}}{N_{\mathrm{Re}}} (1 - N_{VR}) \qquad (14a,b,c,d)$$

$$N_{\mathrm{We}} = -\frac{\omega_3}{\omega_1} \Omega = \lambda\Omega \qquad N_{VR} = \frac{\omega_2}{\omega_3}$$

where N_{Re} is the Reynolds number, N_{We} is the Weissenberg number,[27,30] and N_{VR} is the viscoelastic ratio number. The θ and r velocity components are

$$\frac{v_\theta^{(2)}}{R\Omega} = \frac{N_{\mathrm{Re}}(r^* - 1)}{8r^{*5}} (r^* - 12m) \sin 2\theta \qquad (15a)$$

$$\frac{v_r^{(2)}}{R\Omega} = \frac{N_{\mathrm{Re}}(r^* - 1)^2}{8r^{*5}} [(1 - 4m)r^* - 8m] (3 \sin^2\theta - 2). \qquad (15b)$$

The projections of the steam function, eq. (13), are given in Figure 2 after Thomas and Walters.[50]

EXPERIMENTAL

Materials

The polymer studied was a commercial polystyrene (Dow Styron 678). The density is 1.05 g/cm^3 at 25°C. A gel permeation chromatograph[64,65] trace was obtained on the polystyrene which showed it to have a unimodel molecular weight distribution. The column had previously been calibrated with narrow molecular weight distribution polystyrene samples. From the calibration it was shown that the commercial polymer had a number-average molecular weight (M_n) of 80,000 and a weight-average molecular weight (M_w) of 240,000, giving a polydispersity index M_w/M_n of 3. M_z has a value of 570,000.

The styrene ($CH_2CH\ C_6H_5$) solvent used was a high-purity grade manufactured by Eastman Kodak. It was inhibited with 10 to 15 ppm of *tert*-butylpyrocatechol. Its density was 0.90 g/cm^3 at 25°C, and its boiling point was 145.2°C.

The polystyrene–styrene solutions were prepared by mixing at temperatures up to 60°C with a magnetic stirrer. The solutions were then stored for at least two days at 25°C before use. Solutions with concentrations of 15, 20, 25, 30, 35, 43, 50, and 57% wt-% were prepared.

Rheological Measurements

The shear viscosity μ and principal normal stress difference N_1 were determined on solutions of varying concentration and temperature in a Model R16 Weissenberg rheogoniometer. If one presumes a laminar shearing motion between a cone and plate with small cone angle and neglects the disturbances of this type of flow which have been observed by various authors,[10,11,41,66] the shear rate Γ and the shear stress $\sigma_{\phi\theta}$ where ϕ or "1" is thespherical coordinate direction of flow and θ or "2" the direction of shear, are [67,68].

$$\Gamma = \frac{\Omega}{\tan \chi} \tag{16}$$

$$\sigma_{\phi\vartheta} = \sigma_{12} = \frac{3L}{2\pi R^3} = \mu\Gamma \tag{17}$$

where L is the torque, R is the instrument radius, Ω is the rotor angular velocity, and χ is the angle between the cone and plate. The principal normal stress difference may be similarly expressed in terms of the normal force F,

$$N_1 = \sigma_{\phi\phi} - \sigma_{\theta\theta} = \sigma_{11} - \sigma_{22} = \frac{2F}{\pi R^2}. \tag{18}$$

Flow Pattern Measurements

The experimental arrangement for flow pattern observation consisted essentially of an agitator suspended vertically in the center of a bath. Five agitators (sphere, disc, turbine, two screw propellers) were used. Four of the agitators were $^3/_4$ in. in diameter and were placed on a $^3/_{16}$-in. shaft. One of the screw propellers was 2 in. in diameter and had a $^5/_{16}$-in. shaft. The detailed dimensions are summarized in Figure 3. The agitators were connected to a spark-proof driving motor and a speed controller so that the speed could be varied continuously. The rotational speed was controlled by a motor controller GT-21 by G. K. Heller Corp. Floral Park, New York.

The bath used consisted of a glass container with flat faces avoiding optical distortion and 1-gallon capacity, a so-called "gold fish bowl." The ratio of bath width (at its smallest dimension) to agitator diameter was at least 12 for the $^3/_4$-in. agitators. The bath containing the polymer solutions was immersed in a larger water reservoir maintained at 60°C by a recycle-type temprature controller. Generally, at least 1 hr was required to achieve thermal equilibrium.

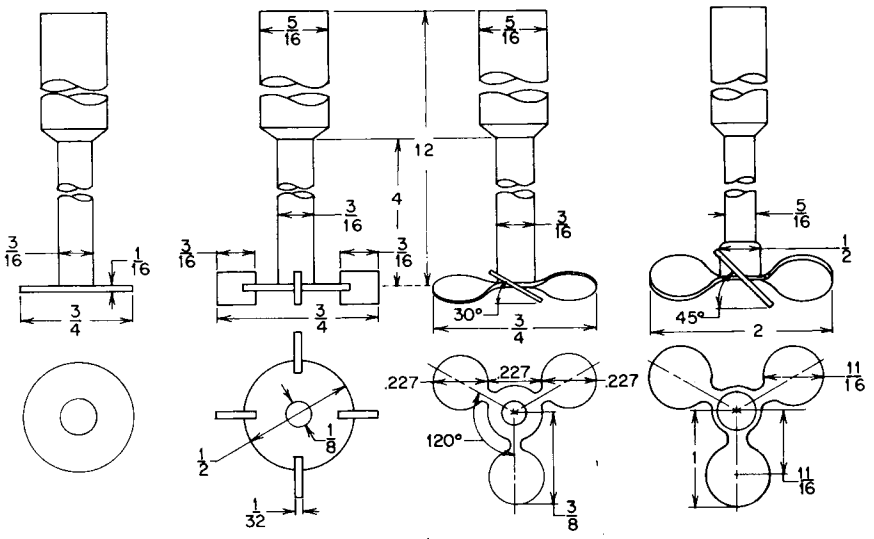

Fig. 3. Detailed dimensions of disc, flat blade turbine, and screw propeller agitators. Dimensions are in inches.

Streamlines were made visible by means of the dye injection technique and then photographed by a Triad Model 70 movie camera. Copies of a film based upon these studies are available by writing to one of us (J.L.W.) The dye was prepared by dissolving "el Marko" by Flair in the styrene. Dye was continuously fed into the transparent solution at the desired place (mainly near the impeller) with the aid of a hypodermic syringe having a sufficiently long needle. The ratio of total dye solution to polymer solution was 0.7 ml to 1 gallon (3.8 liters).

Rotation speeds in the range of 30 to 240 rpm were observed. For the case of the sphere where the fluid mechanics is best understood, this is equivalent to creeping flow shear rates of 9.42 to 75.4 sec^{-1} at the equator of the sphere. This is the maximum shear rate, and it decreases with the third power of the distance from the center of the sphere and the cosine of the angle measured from the equator.

RHEOLOGICAL PROPERTIES

Results

Non-Newtonian shear viscosity μ and first normal stress difference N_1 are plotted as a function of shear rate in Figures 4 and 5. In Figure 4, we plot the variation of viscosity with shear rate for concentrations of 15, 20, 30, 35, 43, 50, and 57 wt-% polystyrene at 60°C. A similar plot of the variation of N_1 versus shear rate for the same concentrations at 60°C is shown in Figure 5. This temperature is still low enough so that there is no spontaneous polymerization. (One may, however, induce polymerization by addition of a free-radical initiator.)

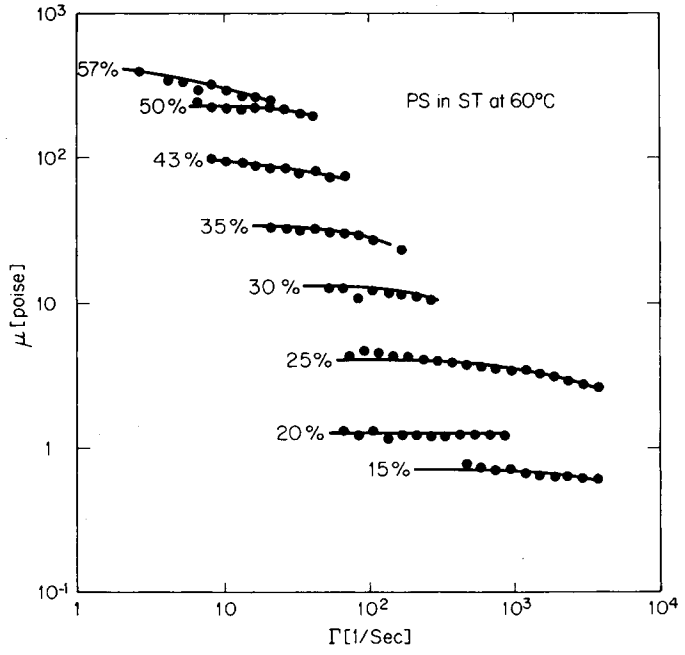

Fig. 4. Viscosity of polystyrene solution of various concentrations at 60°C as a function of shear rate. (The data of 15% and 25% solutions were taken with a smaller cone angle).

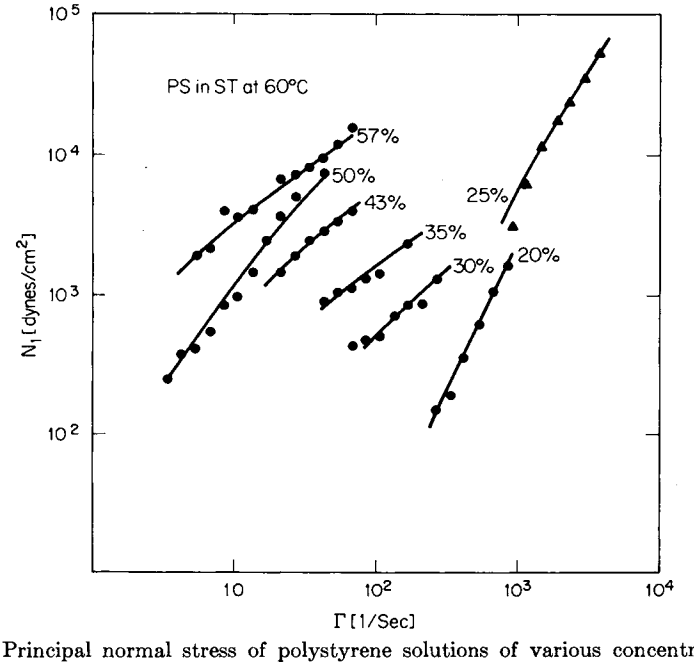

Fig. 5. Principal normal stress of polystyrene solutions of various concentrations at 60°C as a function of shear rate.

The viscosity increases in value with increasing concentration, tending to be Newtonian at low concentrations and shear rates and to be a decreasing function of shear rate at higher concentrations and shear rates.

The principal normal stress difference N_1 is a strongly increasing function of concentration. At low concentrations, it increases with the second power of the shear rate and at a lesser rate in more concentrated solutions. However, the second power dependence of N_1 upon shear rate seems to be a low shear rate asymptote.

Interpretation

The variation of the low shear-rate Newtonian viscosity with concentration is plotted in Figure 6. The data have been fit with the empirical equation

$$\log \eta = A \log c + B. \tag{19}$$

At 60°C, the value of A is about 5.5 and B is 3.85. The observed dependence of viscosity upon concentration is similar to that found by Ferry and his co-workers[69] in early studies on polyisobutylene solutions. More recently, Masuda[40] has found similar dependences to be valid in a wide range of solutions of polystyrene in various solvents. Our concentration dependence data are similar to those found by Nishimura[36] in polystyrene–styrene solutions.

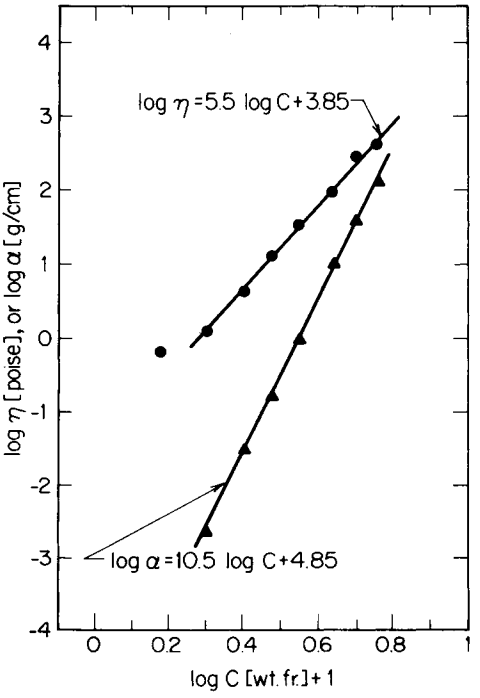

Fig. 6. Zero-shear viscosity η and zero-shear principal normal stress coefficient α plotted against concentration for the polystyrene–styrene solutions.

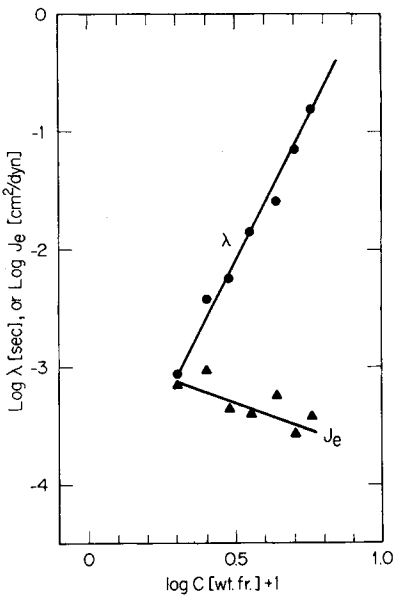

Fig. 7. Characteristic relaxation time λ and the shear compliance J_e plotted against concentration for the polystyrene–styrene solutions.

As we have noted, at low shear rates the principal normal stress difference varies with the second power of the shear rate. We may define a zero-shear normal stress coefficient α analogous to the zero-shear viscosity. The variation of α with concentration is shown in Figure 6. The data may be fit with the logarithmic expression

$$\log \alpha = \log \left[\lim_{\Gamma \to 0} \frac{N_1}{\Gamma^2} \right] = A' \log c + B'. \tag{20}$$

At 60°C, A' is 10.5 and B' is 4.85. Relatively little data relating N_1 to concentration have appeared. Tanner,[70] summarizing existing polyisobutylene data from the literature, finds that α is proportionate to (η/c) to the 1.9th power which could be the 7.6th power if Ferry's viscosity–concentration result is used. Tanner states that this is for cM greater than 8×10^5. Our values of cM are in the range of 0.5×10^5 to 1.4×10^5.

The region of low shear rates where μ is constant and N_1 varies with the second power of the shear rate is the range of second-order fluid response.[25–27] The η of eq. (19) is ω_1, and α of eq. (20) is $(-2)\omega_3$ of second-order fluid theory. The variation of the characteristic relaxation time λ and J_e with concentration may be determined from eq. (5). Clearly, λ varies with about the fifth power of the concentration and J_e with the (-0.5) to (-1.0) power. These results are summarized in Figure 7. The concentration dependence of J_e is similar to that observed by other researchers.[39]

FLOW PATTERNS AROUND ROTATING SPHERE

Predictive Considerations

As the polystyrene–styrene solutions were found to obey or approximate the second-order fluid theory over a reasonably wide range of deformation rates, we should be able to use our rheological data and the hydrodynamic analyses summarized earlier in this paper to quantitatively determine the flow patterns. From eqs. (13)–(15), it may be seen that the key factor in the determination of these flow patterns is the quantity m defined by eq. (14b), which we may rewrite as follows:

$$m = \frac{N_{We}(1 - N_{VR})}{N_{Re}} = \frac{-\omega_3}{\rho R^2}(1 - N_{VR}). \tag{21}$$

The dependence of m upon concentration may be obtained through eq. (20) where we note that α is $(-2)\,\omega_3$. As ω_3 exhibits a 10.5 power concentration dependence, so must m. If we accept a value for N_{VR}, we may make calculations. From eq. (6), we see that N_{VR} is $(-2)\,N_2/N_1$. Based on the experimental studies of various groups[71,72,73] that N_2/N_1 is small and negative, we have taken N_{VR} to be 0.2. The variation of Reynolds number, Weissenberg number, and m with concentration is shown in Figure 8.

It may be seen that when m and polymer concentration are zero, the $v_\theta^{(2)}$ and $v_r^{(2)}$ components are positive. As m increases, the values of the velocity components decrease, go to zero, and become negative. This is

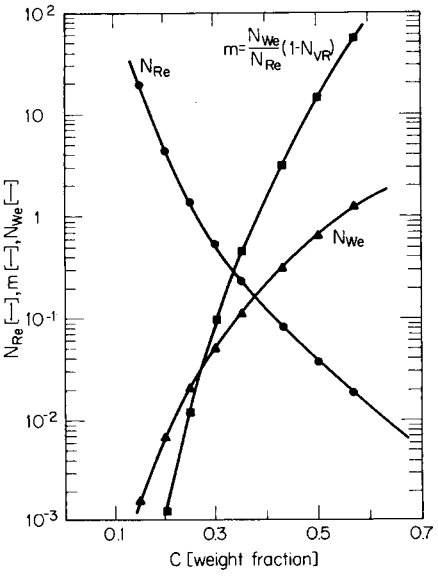

Fig. 8. Reynolds number N_{Re}, Weissenberg number N_{We}, and m (elasticity number as a function of concentration in polystyrene–styrene solutions (Ω = 60 rpm, R = $^3/_8$ in.).

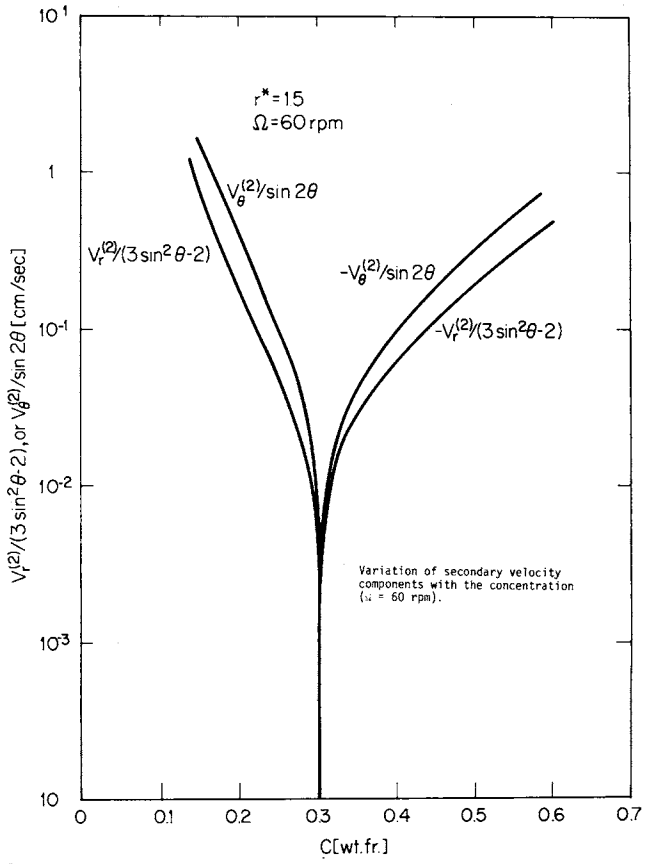

Fig. 9. Predicted variation of secondary velocity components as a function of concentration in the polystyrene–styrene solutions (Ω = 60 rpm, R = $^3/_8$ in.).

illustrated in Figure 9. The $v_\theta^{(2)}$ and $v_r^{(2)}$ of a Newtonian fluid (m = 0) would simply decrease with viscosity. The flow patterns of Figure 2a are indicative of low concentration behavior, Figure 2b, of intermediate and Figure 2c, of high concentration behavior. From Figure 8, we see that the range of concentrations corresponding to Figure 2a is from 0 to 30%, that of Figure 2b, from 30% to 33%, and finally that of Figure 2c corresponds to concentrations greater than 33%.

Giesekus[10] and Walters and Waters[56] have suggested using the flow patterns to determine the m parameter. Actual measurements have been made by Giesekus[10] and Walters and Savins.[12] Giesekus used dye injection techniques to measure $v_r^{(2)}$, while Walters et al. have measured the radius r_s of the sphere encapsulating stagnant regions in Figure 2b. From eq. (15b), we have $v_r^{(2)}$ equal to zero when (for $^1/_4 > m > ^1/_{12}$)

$$r_n^* = \frac{r_s}{R} = \frac{8m}{1 - 4m} \tag{22a}$$

which gives the radius of the equivalent sphere. They also note that for $m > 1/12$, the positions of the nodal points of Figure 2b may be applied to determine m. Specifically,

$$r_n^* = \frac{r_n}{R} = 12m \tag{22b}$$

$$\theta_n = 54°44' \tag{22c}$$

For a 32% solution, we have from Figure 8 that m is 0.18. This could lead us to predict from eq. (22) that there is an equivalent sphere and nodes located at

$$r_s^* = 5.15 \qquad r_n^* = 2.16.$$

For a 57% solution, m is 53. This means that the equivalent sphere has moved out to infinity. The nodes are located at $r_n^* = 636$. This value would only have meaning in a true infinite bath. Under most experimental conditions, there would be wall effects. This point is discussed by Walters and Savins, whose calculations indicate wall effects cause r_n^* to decrease.

Experimental Results

The primary flow observed in polystyrene–styrene solutions about agitators is the same as that seen in water. The primary flow about a sphere is illustrated for water in Figure 10. The secondary flow patterns show considerable variation with concentration. At low concentration (5%, 20%) they resemble those of water. Here, the rotating sphere expels fluid radially outward at the equator. This is shown in Figure 11. At high concentrations, the solution is drawn in at the equator and expelled at the poles, while at intermediate concentrations (30%, 35%) the flow divides into two regions which include segregated vortices in the neighborhood at

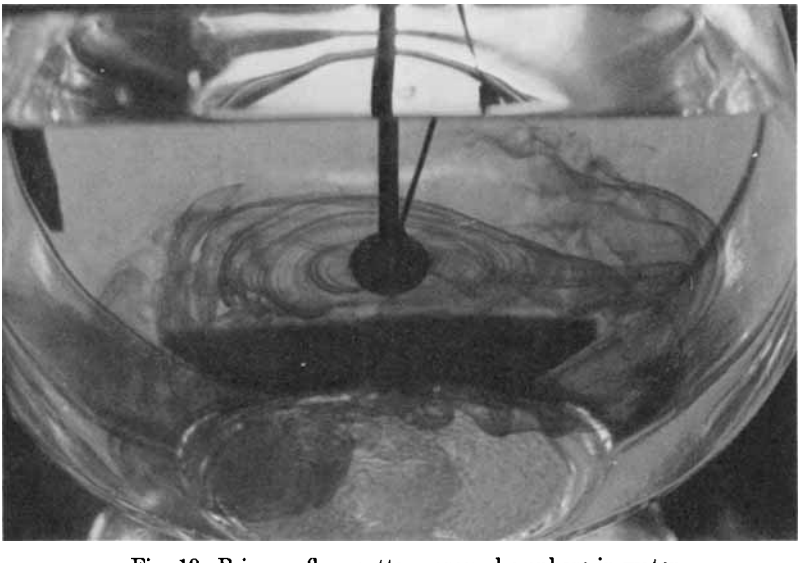

Fig. 10. Primary flow pattern around a sphere in water.

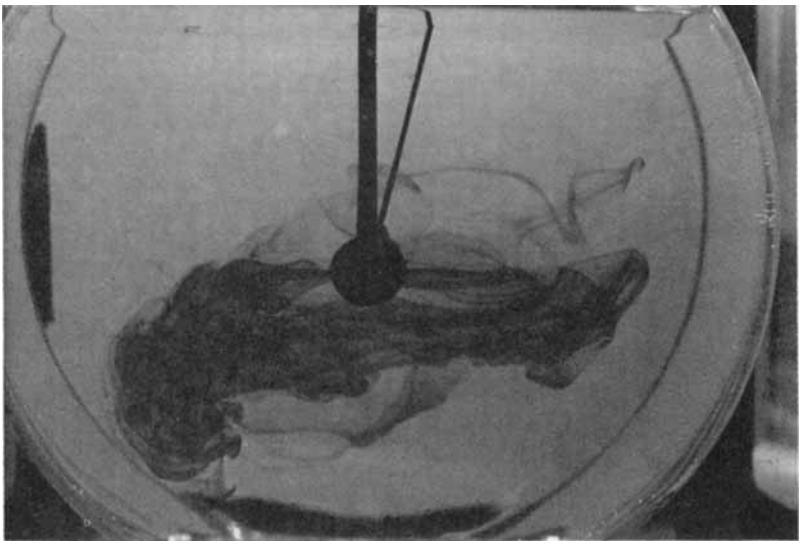

Fig. 11. Secondary flow pattern around a sphere in water.

the sphere. The secondary flow patterns in the intermediate- and high-concentration polystyrene solutions are summarized in Figure 12.

The details of the secondary flow patterns depend upon rotation speed. For the low- and high-concentration solutions, this is largely due to the intensity of the secondary velocities. However, for the intermediate flow pattern case, the size of the stagnant regions increases with rotation speed.

We have made quantitative observations of the flow patterns to compare with the predictions of the second-order fluid theory. For the 32% solution, we observe (at the lower rotation speeds)

$$r_s^* = 6.2 \quad r_n^* = 2.6 \quad \theta_n = 55°$$

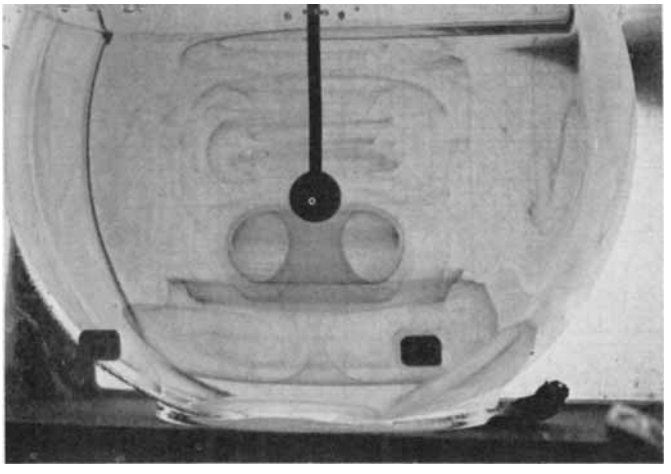

(*a*)

Fig. 12 (*continued*)

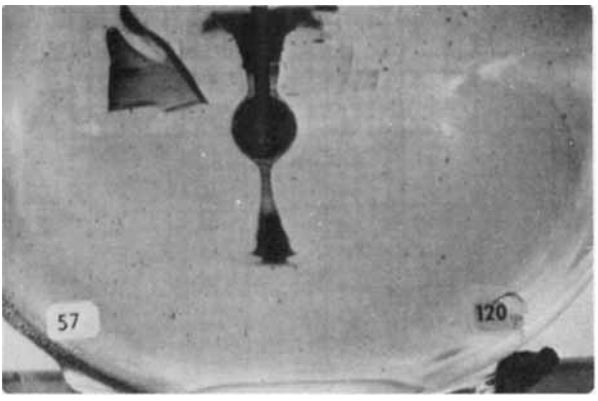

(b)

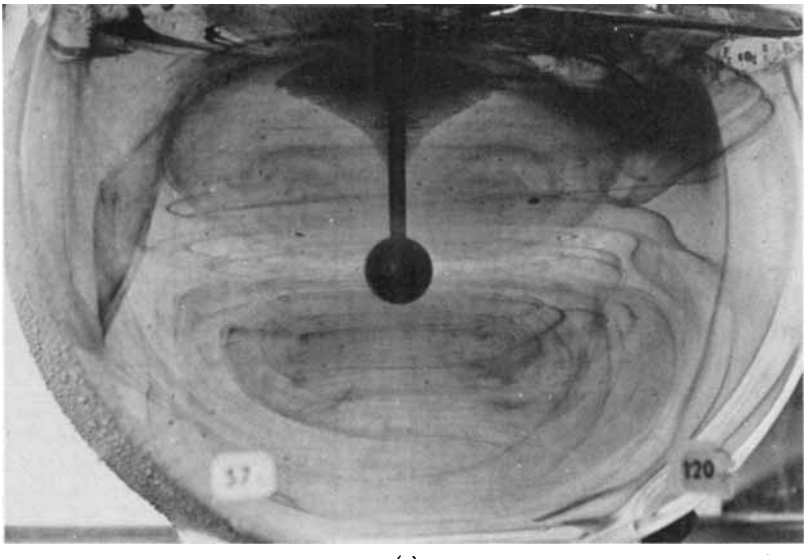

(c)

Fig. 12. Secondary flow patterns in the (a) intermediate (32%) and (b) high (57%) polystyrene concentration, beginning of development, and (c) fully developed.

The agreement of the θ_n values is quantitative. The differences in r_s^* are equivalent to the solution predicting $-\omega_3$ to be 20% higher than measured by the rheogoniometer. For a 57% solution, the sphere has passed to infinity. The position of the nodes are observed at $r_n^* = 3.7$ and $\theta_n = 55°$.

Discussion

The variation of the flow patterns with concentration is very much as predicted by the second-order fluid theory and our rheological data. The m value is predicted to reach the critical region of $^1/_{12}$ to $^1/_4$ corresponding to Figure 2b in the concentration range of 30% to 33%. Our observations indicate that at lower concentrations, fluid is expelled at the equator of the rotating sphere. In this concentration region, segregated flow patterns are

indeed observed. At higher concentrations, fluid is drawn in at the equator and expelled at the poles.

The agreement of the observed flow patterns with theory in the 32% solution must be considered rather good when one considers possible errors in rheogoniometer measurements and the arbitrarily chosen second normal stress difference or viscoelastic ratio number. The error in the 57% solution is more substantial. The angular prediction is correct, but r_n^* is low by a factor of more than 100. This is certainly due to wall effects.

Another point which should be discussed is the sphere rotation rate effect upon the flow patterns. For the 32% solution, both r_s and r_n increase with increasing rotation speed. This is equivalent to an increase in m with increasing shear rate. The answer to this must certainly lie in that, at higher shear rates, additional terms in the acceleration tensor expansion must be included. These will lead to modification of the flow patterns.

FLOW PATTERNS AROUND COMPLEX AGITATORS

Results

As with the spherical agitator, the primary flow field around rotating discs, turbines, and screw propellers studied was essentially that of a Newtonian liquid. The secondary flow patterns differed. For the disc and turbine, the results are qualitatively similar to the sphere. At low concentrations, fluid is expelled radially outward. At high concentrations, the solution flows radially inward and is expelled vertically. At intermediate concentrations (30–35%), segregated secondary flows appear around the agitator. This is summarized in Figure 13 for the flat blade turbine.

The response of the screw propeller agitator is qualitatively different. The action of the screw propeller in a Newtonian fluid is primarily to push the fluid vertically downward in the tank. In the polystyrene–styrene solutions, such response is observed throughout the concentration range studied. The effect is much more pronounced in the 45° screw propeller. It would appear that the normal stress effect reinforces the screw propulsion mechanism.

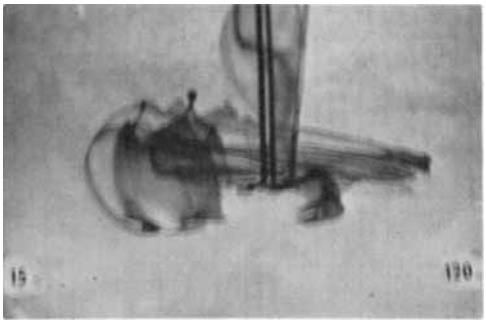

(*a*)

Fig. 13 (*continued*)

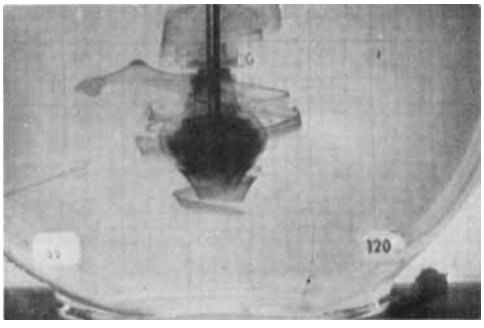

(*b*)

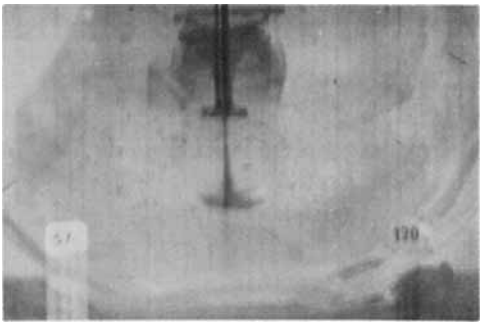

(*c*)

Fig. 13. Flow patterns around a 4 flat blade turbine at (a) 15%, (b) 32%, and (c) 57% polystyrene solution.

Discussion

There are few studies which may be usefully contrasted with those reported in this section. Our flow patterns around turbines at high concentrations are similar to those described by Giesekus[10] on polyacrylamide solutions. The observations of Smith and Peters[13,16–18] on anchor-agitated polymer solutions would seem difficult to compare with our own.

The theoretical analyses of Griffiths, Jones and Walters,[14] and Waters and King[48] may be used as a basis for interpretation of flow patterns around many types of agitators in polymer solutions. From inspecting the solutions of these authors for spheroids and discs, it is apparent that the transition from one flow regime to another occurs at about the same level of rheological properties and thus concentration. We may thus view the observed phenomena as reasonably generally with varying agitator design of the disc-spheroid-turbine type. The fluid mechanics of the screw propeller-type agitator would seem too complex to be interpreted quantitatively.

IMPLICATIONS TO POLYMERIZATION REACTORS

It should be apparent from the experimental study carried out in this paper that during the bulk polymerization of styrene in a batch reactor with

a spheroidal or turbine agitator, the flow patterns around the agitator will show major variations with conversion. At low conversions, the fluid will be expelled radially by the agitator, while at high conversions, the fluid will be drawn in radially and expelled vertically. At intermediate conversions, there will be segregated flow about the agitator. Following the completion of the research described here, we carried out such a bulk polymerization and did observe the three regimes described above.[74] (We hope to report this in detail at a later time.) In a continuous-flow stirred tank reactor (CSTR),[75,76] any of these regimes of flow may exist depending upon the conversion within the reactor.

Methods of manufacture of polystyrene are generally proprietary, though it is usually agreed that much of polystyrene produced is by bulk polymerization. It is thus indeed possible that the phenomena described herein do occur in some commercial polymerization reactors. Interestingly, Goggin[77] in summarizing I. G. Farbenindustrie's methods of polystyrene indicates one commercial process (Type IV) carried out at Ludwigshafen (now B.A.S.F.) which involves a CSTR producing polymer at 33% conversion. This is in the concentration range which one would expect a segregated flow region about the agitator.

The consideration of mixing phenomena in chemical reactions has been dominated by the genius of Danckwerts[78,79] who saw the utility of the concepts of residence time distributions and extent of segregation on a microscopic level. The usefulness of such concepts in chemical reactor behavior has been shown experimentally.[80] This has, however, had the unfortunate effect of a nearly complete neglect of hydrodynamic phenomena in a chemical reactors, as may be seen by surveying monographs in this area.[75,76] Polymerization reactor analyses have generally followed this view[81–84] in spite of the fact that enormous variations in viscosity occur, and the development of viscoelastic character in polymer solutions is well known. The occurrence of autoacceleration at high conversions (concentrations) in free-radical polymerization and the "living polymer" mechanism of anionic polymerization suggest that segregated regions in reactors may lead to distorted molecular weight distributions.[85] Few authors[23,86] have expressed concern over the fluid mechanics of polymerization reactors and then only as an afterthought. We hope this paper helps bring about a change in the "black box type" view.

CONCLUSIONS

1. An experimental study of the rheological properties of a series of polystyrene–styrene solutions of varying concentration has been carried out. Relationships between the zero-shear viscosity and concentration and temperature have been determined. Similar studies have been carried out for the principal normal stress difference N_1. The results have been interpreted in terms of the theory of nonlinear viscoelastic fluids.

2. Flow patterns have been measured about spherical, disc, turbine, and screw propeller agitators in polystyrene–styrene solutions at various concentrations.

3. The flow patterns about the sphere have been compared with predictions of the second-order theory of viscoelastic fluids based upon the rheological property measurements. The agreement is reasonably good.

4. The implication of the observations to the behavior of polymerization reactors has been discussed.

T. Alfrey (Dow Chemical) and K. Walters (University College of Wales) pointed out a number of useful references to the authors.

References

1. E. J. Lyons, *Chem. Eng. Progr.*, **44**, 341 (1948).
2. J. H. Rushton, E. W. Costich, and H. J. Everett, *Chem. Eng. Progr.*, **46**, 395 (1950).
3. J. H. Rushton and J. Y. Oldshue, *Chem. Eng. Progr.*, **49**, 161 (1953).
4. J. P. Sachs and J. H. Rushton, *Chem. Eng. Progr.*, **50**, 597 (1954).
5. S. Nagata, K. Yamamoto, and M. Ujihara, *Chem. Eng. (Japan)*, **23**, 130 (1959); *ibid.*, **24**, 99 (1960).
6. K. W. Norwood and A. B. Metzner, *A.I.Ch.E. J.*, **6**, 432 (1960).
7. J. B. Gray, in *Mixing, Theory and Practice*, V. Uhl and J. B. Gray, eds. Academic Press, New York, 1966.
8. A. DeSouza and R. W. Pike, *Can. J. Chem. Eng.*, **50**, 15 (1972).
9. A. B. Metzner and J. S. Taylor, *A.I.Ch.E. J.*, **6**, 109 (1960).
10. H. Giesekus, *Proc. 4th Int. Rheological Congr.*, **1**, 249 (1965).
11. H. Giesekus, *Rheol. Acta*, **4**, 85 (1965).
12. K. Walters and J. G. Savins, *Trans. Soc. Rheol.*, **9**, 407 (1965).
13. D. C. Peters and J. M. Smith, *Trans. Inst. Chem. Eng.*, **45**, T360 (1967).
14. D. F. Griffiths, D. T. Jones, and K. Walters, *J. Fluid Mech.*, **86**, 161 (1969).
15. D. F. Griffiths and K. Walters, *J. Fluid Mech.*, **42**, 379 (1970).
16. J. M. Smith, *The Chemical Engineer* (March), CE45 (1970).
17. J. M. Smith, *J. Soc. Cosmet. Chem.*, **21**, 541 (1970).
18. D. C. Peters and J. M. Smith, *Can. J. Chem. Eng.*, **47**, 268 (1971).
19. J. V. Kelkar, R. Mashelkar, and J. Ulbrecht, *J. Appl. Polym. Sci.*, **17**, 3069 (1973); *Trans. Inst. Chem. Eng.*, **50**, 343 (1972).
20. R. H. Boundy and R. F. Boyer, *Styrene*, Reinhold, New York, 1952.
21. T. F. Ballenger and J. L. White, *J. Appl. Polym. Sci.*, **15**, 1949 (1971).
22. J. L. White and H. B. Dee, *Polym. Eng. Sci.*, **14**, 212 (1974).
23. R. U. Mehta and J. L. White, *J. Appl. Polym. Sci.*, **16**, 885 (1972).
24. A. E. Green and R. S. Rivlin, *Arch. Rat. Mech. Anal.*, **1**, 1 (1957).
25. B. D. Coleman and W. Noll, *Arch. Rat. Mech. Anal.*, **6**, 355 (1960).
26. B. D. Coleman and H. Markovitz, *J. Appl. Phys.*, **35**, 1 (1964).
27. J. L. White, *J. Appl. Polym. Sci.*, **8**, 1129, 2339 (1964).
28. A. B. Metzner, J. L. White, and M. M. Denn, *A.I.Ch.E. J.*, **12**, 863 (1966).
29. J. L. White and N. Tokita, *J. Appl. Polym. Sci.*, **11**, 321 (1967).
30. D. C. Bogue and J. L. White, *Engineering Analysis of Non-Newtonian Fluids* (in Japanese), translated by N. Mitsuishi and A. Yamanaka Kogyo Chosa Kai, Tokyo (1972) available in English as NATO Agardograph 144, 1971.
31. G. G. Stokes, *Trans. Camb. Phil. Soc.*, **8**, 287 (1845).
32. G. G. Stokes, *Trans. Camb. Phil. Soc.*, **9**, 8 (1851).
33. R. S. Spencer and J. L. Williams, *J. Colloid Sci.*, **2**, 117 (1947).
34. D. J. Streeter and R. F. Boyer, *Ind. Eng. Chem.*, **45**, 1790 (1951).
35. T. Kotaka, M. Kurata, and M. Tamura, *J. Appl. Phys.*, **30**, 1705 (1959); *Rheol. Acta*, **2**, 179 (1962).
36. J. Nishimura, *J. Polym. Sci.*, **A3**, 237 (1965).
37. T. Kotaka and K. Osaki, *J. Poly. Sci.*, **15**, 453 (1966).
38. M. Hirose, E. Oshima, and M. Inoue, *J. Appl. Polym. Sci.*, **12**, 4 (1968).
39. Y. Einaga, K. Osaki, M. Kurata, and M. Tamura, *Macromolecules*, **4**, 87 (1971).

40. T. Masuda, Ph.D. Dissertation, Kyoto University, Kyoto, Japan, 1973.
41. T. Kotaka and J. L. White, *Trans. Soc. Rheol.*, **17**, 587 (1973).
42. G. B. Jeffery, *Phil. Mag.*, **29**, 445 (1915).
43. G. B. Jeffery, *Proc. London Math. Soc.*, **14**, 327 (1915).
44. H. Brenner and R. M. Sonshine, *Q. J. Mech. Appl. Math.*, **17**, 55 (1964).
45. W. G. Bickley, *Phil. Mag.*, **25**, 746 (1938).
46. T. Von Karman, *ZfAMM*, **1**, 244 (1921).
47. S. Goldstein, *Modern Developments in Fluid Dynamics*, Clarendon Press, Oxford, 1938.
48. N. D. Waters and M. J. King, *Q. J. Mech. Appl. Math.*, **24**, 331 (1971).
49. R. Von Mises, *Theory of Flight*, Dover, New York, 1944.
50. R. H. Thomas and K. Walters, *Q. J. Mech. Appl. Math.*, **17**, 39 (1964).
51. W. E. Langlois, *Q. Appl. Math.*, **21**, 61 (1963).
52. A. E. Green and R. S. Rivlin, *Q. Appl. Math.*, **14**, 299 (1956).
53. W. E. Langlois and R. S. Rivlin, *Rend. Mat.*, **22**, 169 (1963).
54. K. Weissenberg, *Nature*, **159**, 130 (1947).
55. M. G. Palekar, *ZAMP*, **16**, 502 (1965).
56. K. Walters and N. D. Waters, *Brit. J. Appl. Phys.*, **14**, 661 (1963); *ibid.*, **15**, 989 (1963).
57. H. Giesekus, *Rheol. Acta*, **6**, 339 (1967).
58. J. M. Kramer and M. W. Johnson, *Trans. Soc. Rheol.*, **16**, 197 (1972).
59. C. T. Hill, *Trans. Soc. Rheol.*, **16**, 213 (1972).
60. E. B. Bagley and A. M. Birks, *J. Appl. Phys.*, **31**, 556 (1960).
61. H. Giesekus, *Rheol. Acta*, **7**, 127 (1968).
62. Y. Tomita and T. Shimbo, *Appl. Polym. Symp.*, **20**, 137 (1973).
63. J. L. White, *Appl. Polym. Symp.*, **20**, 155 (1973).
64. K. Altgeld and J. C. Moore, in *Polymer Fractionation*, M. J. R. Cantow, Ed., Academic Press, New York, 1967.
65. J. L. White, D. G. Salladay, D. O. Quisenberry, and D. L. MacLean, *J. Appl. Polym. Sci.*, **16**, 2811 (1972).
66. R. G. King, *Rheol. Acta*, **5**, 35 (1966).
67. S. M. Freeman and K. Weissenberg, *Nature*, **161**, 324 (1948).
68. S. Middleman, *The Flow of High Polymers*, Interscience, New York, 1968.
69. M. F. Johnson, W. W. Evans, I. Jordan, and J. D. Ferry, *J. Colloid Sci.*, **7**, 498 (1952).
70. R. I. Tanner, *Trans. Soc. Rheol.*, **17**, 365 (1973).
71. R. F. Ginn and A. B. Metzner, *Trans. Soc. Rheol.*, **13**, 429 (1969).
72. M. J. Miller and E. B. Christiansen, *A.I.Ch.E. J.*, **18**, 600 (1972).
73. O. Olabisi and M. C. Williams, *Trans. Soc. Rheol.*, **16**, 727 (1972).
74. Y. Ide and J. L. White, unpublished research, 1972–73.
75. O. Levenspiel, *Chemical Reaction Engineering*, Wiley, New York, 1962.
76. R. Aris, *Introduction to the Analysis of Chemical Reactors*, Prentice-Hall, Englewood Cliffs, 1965.
77. W. C. Goggin, in *Styrene*, R. H. Boundy and R. F. Boyer, Eds., Reinhold, New York, 1952.
78. P. V. Danckwerts, *Chem. Eng. Sci.*, **2**, 1 (1953).
79. P. V. Danckwerts, *Chem. Eng. Sci.*, **8**, 93 (1958).
80. N. Mitsuishi, K. Nakano, and Y. Ide, *J. Chem. Eng. Japan*, **5**, 407 (1972).
81. K. G. Denbigh, *Trans. Faraday Soc.*, **43**, 648 (1947).
82. Z. Tadmor and J. A. Biesenberger, *Ind. Eng. Chem., Fundam.*, **5**, 336 (1966).
83. J. C. Mecklenburg, *Can. J. Chem. Eng.*, **48**, 279 (1970).
84. W. H. Ray, *J. Macromol. Sci.*, **C8**, 1 (1972).
85. R. W. Lenz, *Organic Chemistry of Synthetic High Polymers*, Interscience-Wiley, New York, 1967.
86. S. Lynn and J. E. Huff, *A.I.Ch.E. J.*, **17**, 475 (1971).

Received March 8, 1974
Revised April 9, 1974